Status of the Low-Cost Radiator for Fission Surface Power

Taylor Maxwell[1], Calin Tarau[2], William G. Anderson[3] and Scott Garner[4]
Advanced Cooling Technologies, 1046 New Holland Ave. Lancaster PA 17601

Matthew Wrosch[5]
Vanguard Space Technologies, Inc., San Diego, CA 92126

Maxwell H. Briggs[6]
NASA Glenn Research Center, Cleveland, OH, 44135

NASA Glenn Research Center (GRC) is developing fission power system technology for future Lunar surface power applications. The systems are envisioned in the 10 to 100kWe range and have an anticipated design life of 8 to 15 years with no maintenance. NASA GRC is currently setting up a 55 kWe non-nuclear system ground test in thermal-vacuum to validate technologies required to transfer reactor heat, convert the heat into electricity, reject waste heat, process the electrical output, and demonstrate overall system performance. Reducing the radiator mass, size, and cost is essential to the success of the program. To meet these goals, Advanced Cooling Technologies, Inc. (ACT) and Vanguard Space Technologies, Inc. (VST) are developing a single facesheet radiator with heat pipes directly bonded to the facesheet. The facesheet material is a graphite fiber reinforced composite (GFRC) and the heat pipes are titanium/water. By directly bonding a single facesheet to the heat pipes, several heavy and expensive components can be eliminated from the traditional radiator design such as, POCO™ foam saddles, aluminum honeycomb, and a second facesheet. The paper presents the final design of the full-scale modular radiator as well as the status of the direct bond and radiator module development.

I. Introduction

NASA Glenn Glenn Research Center (GRC) is developing fission power system technology for future Lunar surface power applications. The systems are envisioned in the 10 to 100kW$_e$ range and have an anticipated design life of 8 to 15 years with no maintenance. A nominal lunar fission surface power design has been developed and is shown in Figure 1 (Mason, Poston, and Qualls, 2008). The nuclear reactor supplies thermal energy to Brayton (or Stirling) convertors to produce electricity, and uses a heat pipe radiator to reject the waste heat generated by the convertors. The radiator panels must reject heat from both sides to achieve the highest efficiency; therefore, the optimum mounting position is vertical. The radiator panels contain embedded heat pipes to improve thermal transfer efficiency. Since the heat pipe evaporator is on the bottom, the heat pipes are gravity aided and can work as a thermosyphon. This is advantageous because the heat pipe is not required to pump the working fluid back to the evaporator against gravity. Heat is supplied to the heat pipes through a titanium/water heat exchanger that is coupled with the coolant loop in the radiator.

Currently, NASA GRC is putting together a Fission Power System Technology Demonstration Unit (TDU) (Mason et al., 2012, Briggs et al., 2015). The TDU is a non-nuclear demonstration unit that will be tested in thermal-vacuum to demonstrate integrated system performance. The primary goals for the early systems are low cost, high reliability and long life. To help achieve these goals, ACT, NASA GRC and VST are developing a single facesheet direct-bond radiator; see Figure 2. The radiator will have Variable Conductance Heat Pipes (VCHPs) made from titanium and will use water as the working fluid.

---

[1] R&D Engineer, Defense and Aerospace Products, 1046 New Holland Ave.
[2] Lead Engineer, Principal Investigator, Defense and Aerospace Products, 1046 New Holland Ave.
[3] Chief Engineer, 1046 New Holland Ave, AIAA Member
[4] Manager , Defense and Aerospace Products, 1046 New Holland Ave.
[5] Principal Investigator, 9431 Dowdy Drive
[6] Program Manager, 21000 Brookpark Road

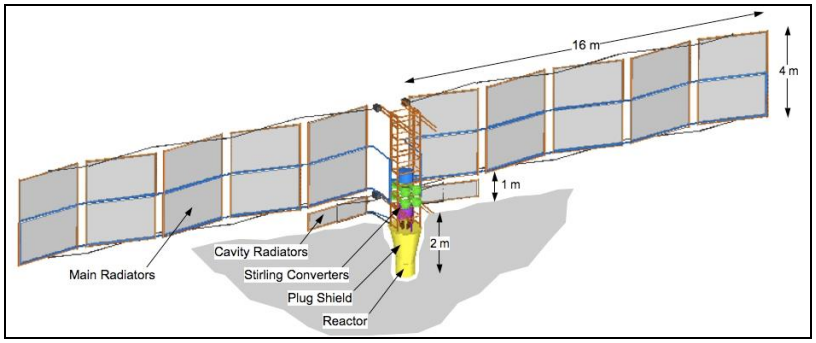

Figure 1. Fission surface power system concept (Mason, Poston, and Qualls, 2008).

Currently, NASA GRC is putting together a Fission Power System Technology Demonstration Unit (TDU) (Mason et al., 2012). The TDU is a non-nuclear demonstration unit that will be tested in thermal-vacuum to demonstrate integrated system performance. The primary goals for the early systems are low cost, high reliability and long life. To help achieve these goals, ACT, NASA GRC and VST are developing a single facesheet direct-bond radiator (see Figure 2). The radiator will have Variable Conductance Heat Pipes (VCHPs) made from titanium and will use water as the working fluid.

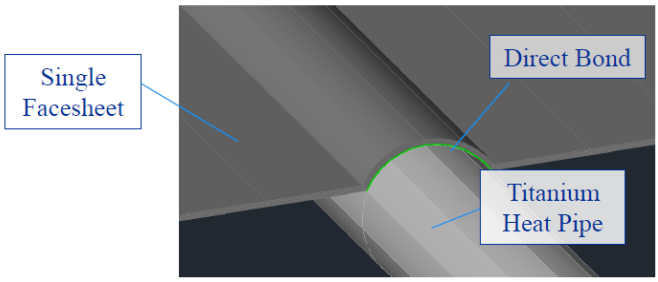

Figure 2. Single-facesheet radiator with direct bonding of the facesheet to the heat pipes. (Briggs, 2012)

II. Background on Variable Conductance Heat Pipe Radiators

A. Heat Pipe and Radiator Materials for Surface Fission Power

Heat pipe spacecraft radiators typically have grooved aluminum/ammonia heat pipes to transfer the heat, with aluminum facesheets to radiate the heat to space. These radiator panels are used to cool the spacecraft electronics, and operate best at temperatures below about 300 K. Their maximum operating temperature is roughly 330 K, with significantly reduced carrying capacity. On the other hand, the surface fission power designs reject heat in the roughly 375 to 400 K range, so a different heat pipe envelope and working fluid must be used. ACT identified water as the best working fluid in this temperature range. Aluminum is incompatible with water, and can't be used in the heat pipe. Most water heat pipes have a copper working fluid and wick, but this is too heavy for fission power application, particularly some early fission surface power designs, with the heat pipes operating at temperatures up to 550 K.

ACT identified titanium, titanium alloys, Monel 400, and Monel K500 as potential heat pipe envelope materials that should be compatible with water. For the past ten years, long term heat pipe life tests with water and these materials were carried out, and the long term compatibility has been demonstrated (Anderson et al., 2013a). Since titanium and its alloys are lighter than Monel, titanium has been chosen for the heat pipe alloy and wick.

The radiators will go through large temperature swings, so must be able to accommodate any Coefficient for Thermal Expansion (C.T.E.) mismatch between the radiator panels and the heat pipes. Titanium has a C.T.E. of about 8.6 µm/m °C, while the aluminum the standard radiator facesheet material, has a much higher C.T.E., 22.2 µm/m °C. Since this large C.T.E. difference could have caused problems, ACT and VST examined different potential materials, and chose Graphite Fiber Reinforced Composite (GFRC) laminates for the radiator facesheets. (Stern and Anderson, 2005).

One of the advantages of GFRC laminates is that the layup of the GFRC plies can be adjusted to match the titanium C.T.E. along the heat pipe axis. In the perpendicular direction, the C.T.E. of the GFRC facesheet is

actually less than zero (-1.1 µm/m °C), to the facesheet actually shrinks in this direction as it heats up. The heat pipe radiator design must accommodate this mismatch.

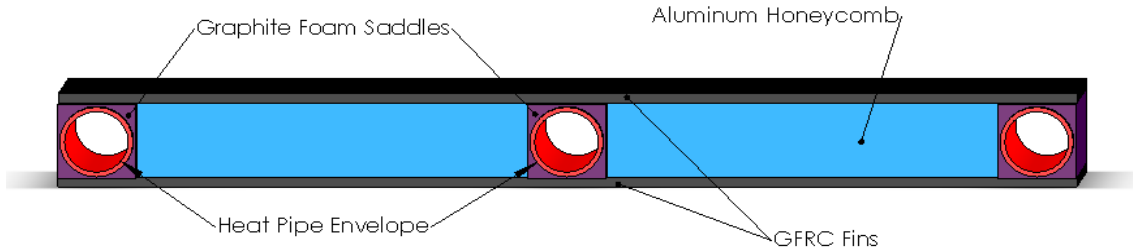

Figure 3. Cut-away section through the radiator panel.

The initial radiator design was based on the standard aluminum radiator, which has lightweight conductive facesheets and a honeycomb core. The heat pipe configuration assumes that a series of round heat pipes are embedded in the radiator panel to distribute heat. Aluminum/ammonia heat pipes are typically fabricated with an integral saddle that is used to transfer heat from the heat pipe to the radiator panel. This is not suitable for a titanium heat pipe, for two reasons:

1. Titanium is difficult to extrude
2. Unlike aluminum, the thermal conductivity of titanium is very low. The titanium thickness is minimized to minimize the temperature drop from the heat pipes to the fin.

Instead, the radiator panel has the following (Anderson et al., 2006):

1. A series of titanium/water heat pipes to transfer heat from the secondary fluid to the radiator panel
2. High conductivity POCO foam graphite saddles to form an interface between the circular heat pipe and the flat fin
3. High conductivity fins
4. Aluminum honeycomb to provide stiffness to the structure

The initial Radiator Demonstration Unit (RDU) panel is shown in Figure 4. The panel had three free-floating heat pipes, so that only the C.T.E. mismatch between a heat pipe and the panel had to be accommodated. In the next interation, discussed below, the design was changed to accommodate the C.T.E. mismatch between multiple plates, and used Variable Conductance Heat Pipes.

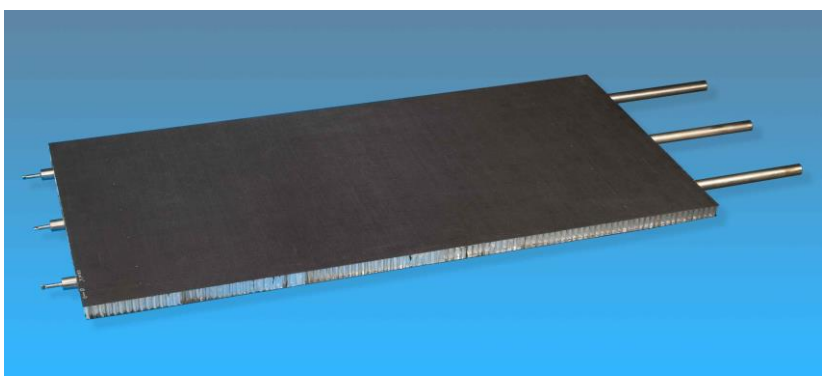

Figure 4. Initial RDU radiator panel with three titanium/water heat pipes, and a GFRC composite fin. The panel is 1 m by 0.5 m, and has graphite foam saddles to accommodate the C.T.E. mismatch, and aluminum honeycomb for stiffness.

B. VCHP Radiators for Lunar and Martian Surface Fission Power

Variable Conductance Heat Pipes (VCHPs) aid in start-up/shut-down, as well as passively limiting the evaporator temperature range during varying heat load or changing sink temperature conditions. A simple VCHP is shown below in Figure 5. It is similar to a conventional heat pipe but has a reservoir and controlled amount of non-condensable gas (NCG) inside the reservoir. When the heat pipe is operating, the NCG is swept toward the condenser end of the heat pipe by the flow of the working fluid vapor. The NCG then blocks the working fluid from reaching a portion of the condenser. The VCHP works by varying the amount of condenser available to the working

fluid. As the evaporator temperature increases, the vapor temperature (and pressure) rises, which compresses the NCG (Figure 5 top) and thus more condenser is exposed to the working fluid. This increases the effective conductivity of the heat pipe and drives the temperature of the evaporator down. Conversely, if the evaporator cools, the vapor pressure drops and the NCG expands (Figure 5 bottom). This reduces the amount of available condenser, decreases the effective heat pipe conductivity, and increases the evaporator temperature.

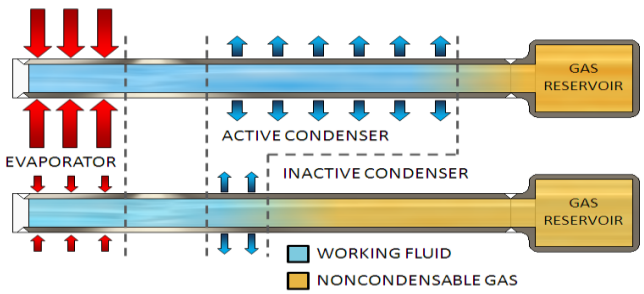

Figure 5. The working of a VCHP is illustrated. At high heat load, the temperature dependent saturation pressure of the working fluid is high and compresses the NCG into the reservoir. At lower heat input the working fluid temperature and pressure is lower, and the non-condensable gas expands into the condenser.

ACT developed a traditional VCHP radiator for fission surface power applications under a previous NASA SBIR Phase II program; see Figure 6a (Anderson et al., 2013). A full-scale radiator panel was designed, fabricated and tested during the Phase II program. This included thermal performance testing in a vacuum at NASA GRC. The full-scale panel utilized five VCHPs embedded in POCO™ foam saddles and two Graphite Fiber Reinforced Composite (GFRC) facesheets epoxied to either side of the saddle. Aluminum honeycomb was then used as a stiffener to fill the void space between VCHP/foam saddle assemblies. A top down view of the VCHP radiator can be seen in Figure 6b.

.

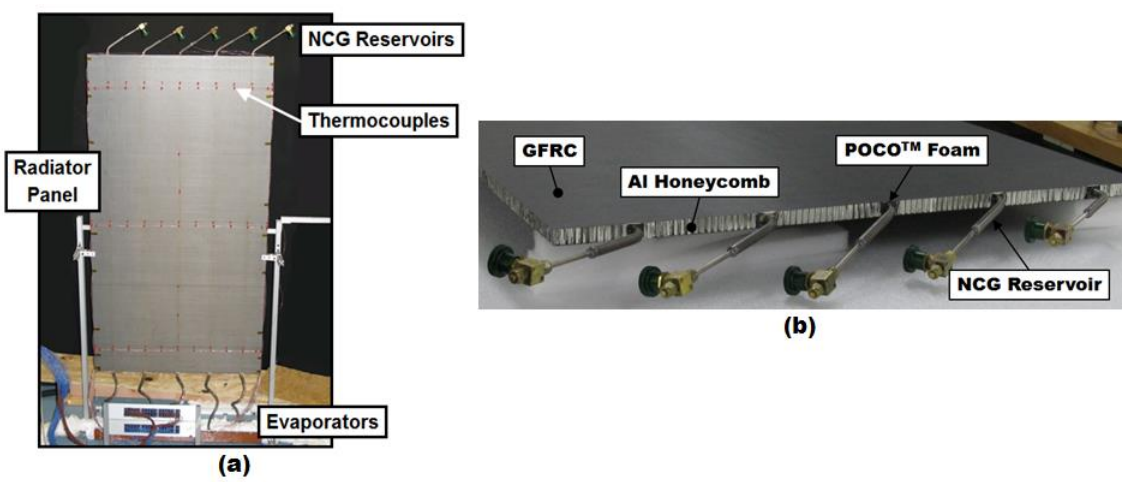

Figure 6. a) VCHP radiator in testing configuration, b) cross section of VCHP radiator

The radiator panel was designed to operate in the 370 to 400K temperature range and uses a novel evaporator design to integrate with the fission reactor coolant manifold. The use of embedded VCHPs instead of Constant Conductance Heat Pipes (CCHPs) allowed the radiator to operate over a wide range of sink conditions and also enabled the radiator panel to start up from a frozen state. The temperature on the lunar surface can vary from 50K during lunar night to 330K during lunar day. The variable conductance nature of the VCHP radiator allows the system to reject heat during the lunar day, and adjust the heat rejection during the lunar night with the colder heat sink. This is achieved through the use of a non-condensable gas (NCG) located in a reservoir at the end of the VCHP condenser. As ambient temperatures begin to decrease, so does the operating temperature of the working fluid contained within the VCHP. This decrease in temperature causes the vapor pressure of the working fluid to also decrease and allows the NCG contained in the reservoir to expand, reducing the effective length of the condenser. Conversely, as the ambient temperature begins to increase, the operating temperature and vapor pressure

of the working fluid increases. This results in compression of the NCG into the reservoir and increases the effective length of the condenser.

Unlike the earlier RDU panel (Figure 4), this heat pipes in this radiator panel have a coiled adiabatic section, to accommodate the C.T.E. mismatch (Anderson et al., 2013). This allowed the radiator panel in Figure 6 to be tied into a titanium/pumped loop, with relevant flow rates for the Lunar Fission Surface Power Radiator in Figure 1.

Radiator Panel Mechanical Strength

During the development of the VCHP radiator, VST built a small, non-operational two-pipe radiator panel for mechanical strength testing. The panel was constructed in order to verify that the pipes would not shear from the radiator panels when exposed to forces perpendicular to the heat pipe axis; see Figure 7.

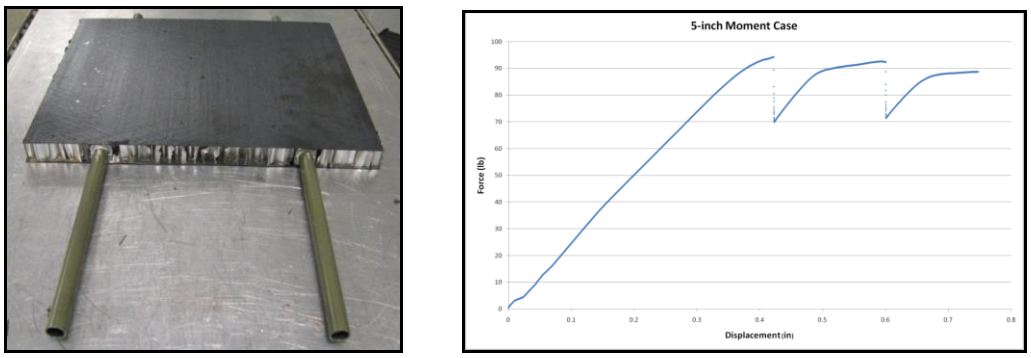

Figure 7. a) Two-pipe mechanical-strength test panel and b) Force versus displacement

The panel was more robust than expected. When the forces were applied to the tube with a 5" moment, the POCO withstood ≈42kgf with nearly 0.4" displacement. During the 5" moment test, the pipe began to deform plastically, indicated by the discontinuities on the curve. The effect of the bending of the titanium pipe dominated the test results. Thus, the pipe will bend before the radiator panel fails. POCO foam is expensive and difficult to machine. In addition, it adds significant mass to the overall radiator. The above mechanical tests indicated that it may be possible to eliminate the POCO foam saddles, and bond the facesheet directly to the titanium heat pipe.

C. Single Facesheet Radiator Proof of Concept

Figure 2 illustrates the concept of the single, direct bond radiator. The single, direct-bond facesheet radiator has the advantages of reducing mass and cost of the system by eliminating the graphite foam saddles, aluminum honeycomb, and one of the graphite fiber reinforced composite (GFRC) facesheets, which are present in the previouse ACT/VST heat pipe radiators. ACT and VST have previously demonstrated the feasibility of the single facesheet radiator by fabricating and testing small-scale, two heat pipe radiator panel (Maxwell et al., 2014).

III. Status of the Low-Cost for Surface Fission Power Radiator Development

D. Full Scale Radiator Final Design

The analytical model developed in the Phase I program used to size the radiator and determine thermal performance at nominal conditions was upgraded and further validated at the module level. Once the validity of the model was confirmed, a brief trade study was conducted to down-select to the final radiator design. This trade study only focused on two aspects: the effect of condenser outer diameter on the thermal performance of the radiator (seen in Figure 8) and the radiator performance as a VCHP for various waste heat loads at 250 K sink temperature (Figures 9 and 10). All other design parameters were down-selected in the Phase I trade study (Maxwell, Tarau, Anderson, Wrosch, and Briggs, 2014).

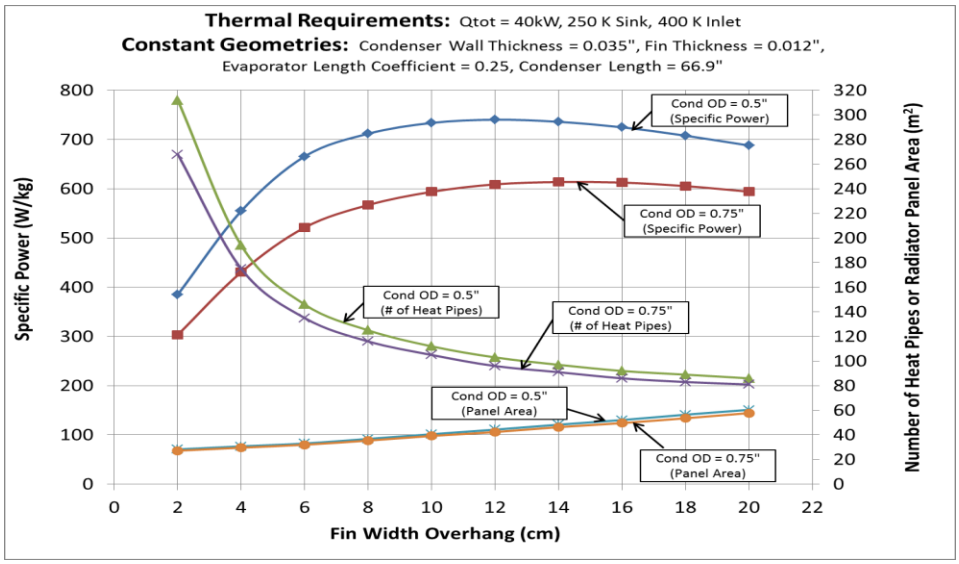

Figure 8. Effect of fin width overhang outer diameter on specific power for 0.5 and 0.75 in. condenser outer diameters

From Figure 9 it is clear that the 0.5 in. condenser design has a significantly higher specific power per unit fin width compared to the 0.75 in. design. However, it was determined that the specific power was not the most important design factor, since this radiator is not intended for flight applications. Ultimately, it was decided that the 0.75 in. condenser design was more suitable for TDU integration, since it lowers the risk of composite fiber breakage during facesheet bonding and also allows for more heat transfer area between the pipes and facesheet lowering the thermal resistance, thus reducing the necessary number of heat pipes (radiator modules). Table 1 summarizes the mass and thermal performance of the final radiator design.

Table 1. Summary of final radiator design

Geometry	0.75" Cond. OD Design
Evaporator Length (cm)	13
Adiabatic Section Length (cm)	7.62
Condenser Length (cm)	170
NCG Reservoir Length (cm)	7.62
Fin Width Overhang (cm)	12
Total GFRC Area (m^2)	42.36
Total Number of Heat Pipe Modules	96
Total Number of Heat Pipe Clusters	12
Heat Pipe Redundancy Compared to Nominal Radiator (i.e. 36kW, 175K Sink, 400K inlet)	23
% Margin by Area Compared to Nominal Radiator	24
Thermal Performance & Mass	
Total Power Output (kW)	40
Specific Power (W/kg)	609.0
Dry Mass of Single Heat Pipe/Fin Module (kg)	0.685
Total Dry Mass of Radiator System (kg)	65.74

VCHP feature

In addition, the radiator model was also outfitted with a modular VCHP model to determine the radiator's ability to accommodate variable power and sink temperature conditions. The VCHP model was based on the flat front theory and assumed a constant reservoir length for all heat pipes. The amount of NCG was also assumed constant and was calculated based on the vapor temperature of the coldest heat pipe during the hottest expected conditions during TDU operation (40 kW, 400 K radiator inlet, 250 K sink). By sizing the amount of NCG vapor for the

hottest sink condition, all condensers are assured to be fully active during the hot conditions with the NCG front pushed deeper into the reservoir for the hotter (i.e. upstream) heat pipes. Since it is expected that the power control unit (PCU) will reject a constant heat load during steady state conditions, the VCHP model allows the user to predict how much the water supply temperature will have to adjust to accommodate the prescribed heat load. The VCHP performance plots for the final radiator design for various waste heat loads rejected to sink of constant temperature of 250 K and 175 K are shown in Figure 9a and b respectively.

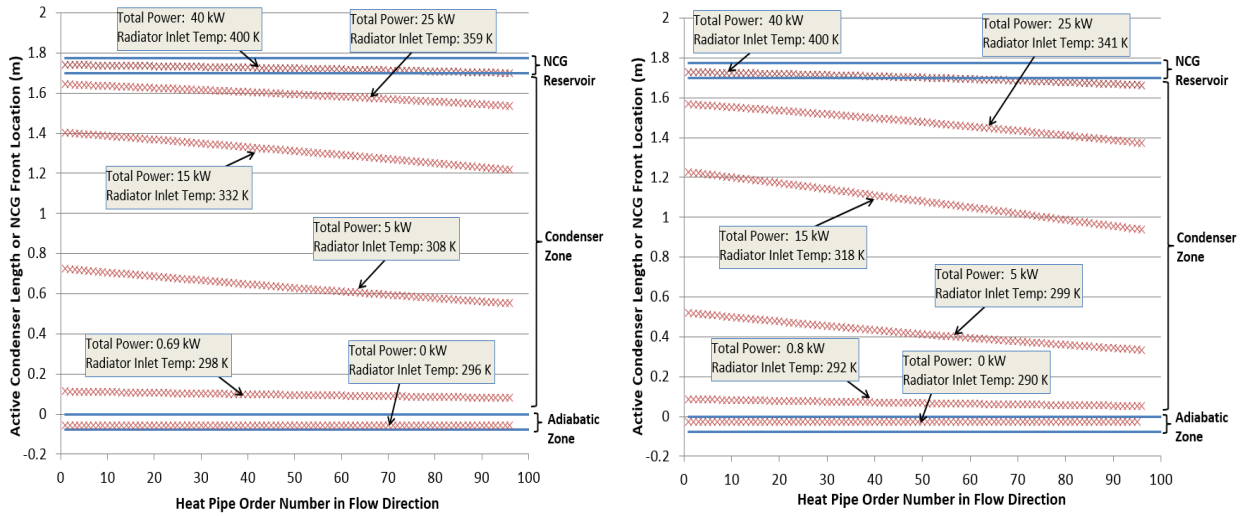

Figure 9. VCHP performance results for final radiator design for various waste heat loads at a) 250 K and b) 175 K sink temperature

Figure 9a shows how the NCG front location varies along the radiator in the direction of coolant flow for various waste heat loads for the worst case sink temperature (250 K). As the waste heat load decreases from the maximum expected value of 40 kW, the NCG front gradually blocks portions of the radiator to increase thermal resistance. Figure 9b shows similar results for a sink temperature of 175 K.

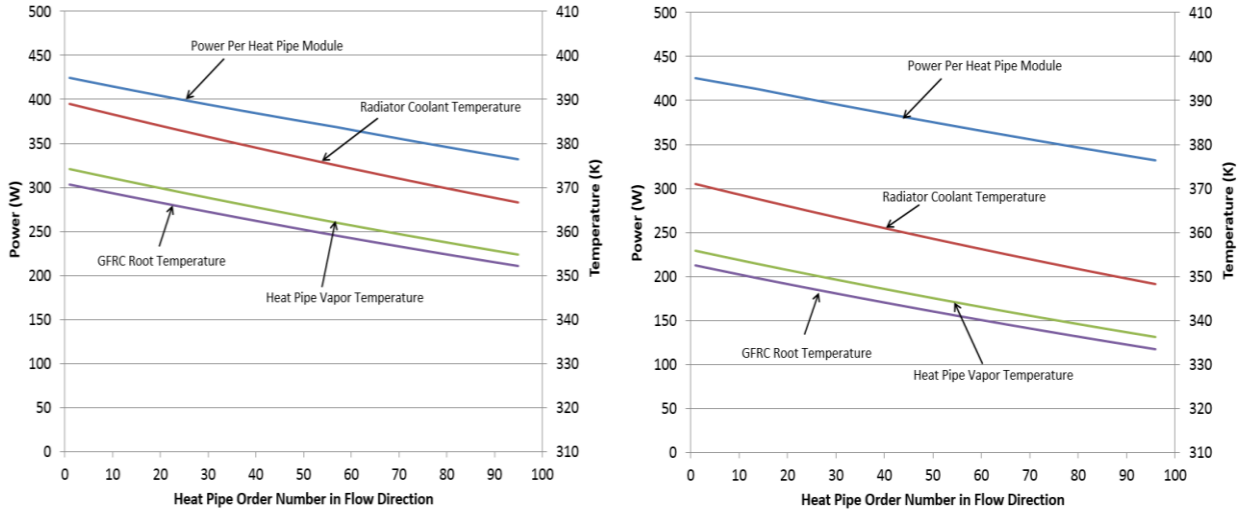

Figure 10. VCHP power and temperature distribution for final radiator design at 36 kW output with a) 250 K sink with 389 K radiator inlet temperature and b) 175 K sink with 371 K radiator inlet temperature

Figure 10 shows the power and temperature distribution for the final radiator design for two different operating conditions: a) nominal power output of 36 kW and hot sink conditions (250 K) and the same nominal power output

and cold conditions (175 K). As seen, the inlet temperatures had to be adjusted accordingly to 389 K and 371 K respectively.

E. Full-Scale Module Development

As previously presented the design of the full scale radiator is modular where one module consists of a heat pipe that is attached to one independent GFRC fin. The core of full scale radiator development is the module development and it is presented in this section of the paper. To be noted is that the fabricated module testing results are not presented in this paper since the fabrication was not completed by the time of writing the paper.

Direct-Bond Development

The main challenge during the module development task is the direct-bond attachment of the GFRC fin to the titanium heat pipe condenser. The original intent was to screen two different types of adhesives (FM300-2U Film and BF522 Film), as well as to investigate a co-cure method for direct bonding the composite prepreg to the titanium. However, it was determined that a significant amount of tooling was required to co-cure flat geometry lap shear samples. Therefore, only the two film adhesives were screened.

Lap shear fingers come in sets of four, and for each material set there will be two sets of four fingers, or 8 total for each set, for a total of 16 samples. This number of samples allowed for the determination of b-basis allowables for each configuration. Fracture surfaces were analyzed for the mode of failure and the lap-shear strengths are summarized in Figures 9a and 9b below.

Specimen #	Width (in.)	Length (in.)	Bondline Thickness (in.)	Peak Load (lbf)	Peak Stress (psi)
1	0.998	0.988	0.0040	901.418	913.7
2	0.998	0.998	0.0040	732.641	735.2
3	1.000	0.988	0.0045	801.623	811.8
4	1.000	0.988	0.0043	837.905	848.1
5	0.999	0.988	0.0035	615.461	623.9
6	1.000	0.988	0.0035	884.863	895.6
7	0.998	0.988	0.0035	851.261	862.5
8	0.999	0.988	0.0045	945.502	958.4
9	0.999	0.988	0.0045	804.864	815.9
Mean	0.999	0.989	0.0040	**819.504**	**829.4**
Std. Dev	0.001	0.003	0.0004	**98.690**	**100.7**

a)

Specimen #	Width (in.)	Length (in.)	Bondline Thickness (in.)	Peak Load (lbf)	Peak Stress (psi)
1	0.998	0.988	0.0040	672.850	682.4
2	0.998	0.988	0.0040	561.135	569.1
3	0.998	0.988	0.0040	661.416	670.1
4	0.998	0.988	0.0040	667.613	677.1
5	0.998	0.988	0.0040	571.075	578.9
6	0.999	0.988	0.0040	617.677	625.5
7	0.999	0.988	0.0040	618.166	626.3
8	1.000	0.988	0.0040	571.941	579.0
9	0.998	0.988	0.0040	591.406	599.2
Mean	0.999	0.988	0.0040	**614.809**	**623.1**
Std. Dev	0.000	0.000	0.0000	**44.056**	**44.8**

b)

Figure 11. Lap-shear results using a) FM300-2U and b) BF522 film adhesive at room temperature

Overall, both film adhesives performed well. All failures observed were interlaminar (i.e. composite failure). However, the FM300-2U demonstrated slightly higher performance compared to the BF522. This may have been the result of a higher cure temperature required for BF522, which could have compromised the interlaminar shear strength of the composite laminate. As a result, it was decided to eliminate the BF522 from scope and further investigate the shear strength of the FM300-2U at elevated temperatures (~130°C). However, the high temperature testing results were inconclusive. Primer failure at the titanium to adhesive interface was present on some coupons which resulted in a large standard deviation.

Direct Bonding Channel-Depth Optimization

A manufacturing risk-reduction effort was implemented at VST prior to machining the production radiator cluster tooling to evaluate an optimum channel-depth and maximize interfacial (thermal) contact between the heat pipe and the composite while retaining continuity among the fibers. Shown in Figure 12 is the schematic of three short titanium heat pipes where both the contact angle between the heat pipe and the GFRC radiator and the depth of the radiator wrap are varied. The fabricated heat pipe radiator sections are shown in Figure 13.

The lowest risk design is the 0.0” depth and 119° contact angle. The wrap depth is measured from the centerline of the pipe. The other two options were increased radiator panel wrap depths of 0.100” and 0.200” below the pipe centerline. Each heat pipe is 24 inches long and the radiator panel is 17 inches long and 9.45 inches wide.

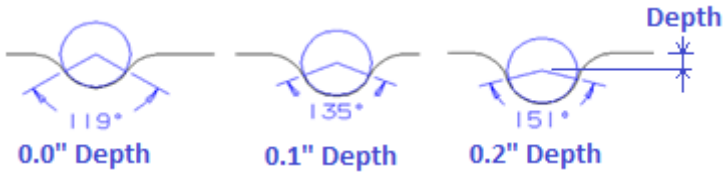

Figure 12. Schematic showing the variation of the contact angles and depths associated with the adhesive bond geometry that were be evaluated

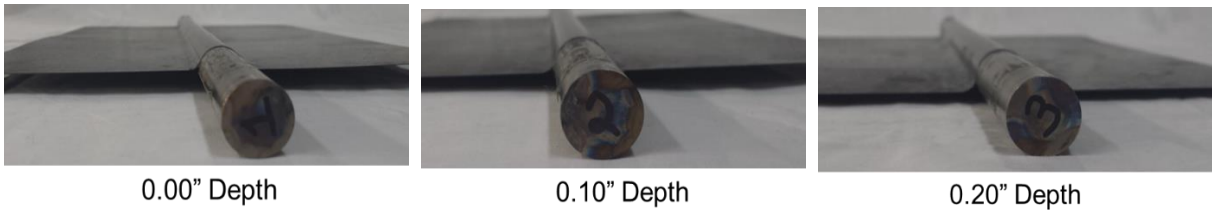

Figure 13. Fabricated short heat pipe radiator sections

The three heat pipe radiator samples were designed and manufactured to be as identical as possible in order to accurately compare the performance of each radiator design. The three assemblies were thermally tested in both air and vacuum to evaluate thermal performance and uniformity of the adhesive bond between the radiator panel and the heat pipe. The orientation during testing was vertical for all three pipes. Heat was applied to the evaporator section using a heater block with four electric cartridge heaters. Thermocouples were installed on the heat pipe and GFRC panel to evaluate the thermal performance of each radiator design. Additionally a thermal imaging camera was employed to measure uniformity of the bond. The instrumented heat pipe as it was tested in the vacuum chamber is shown in Figure 14.

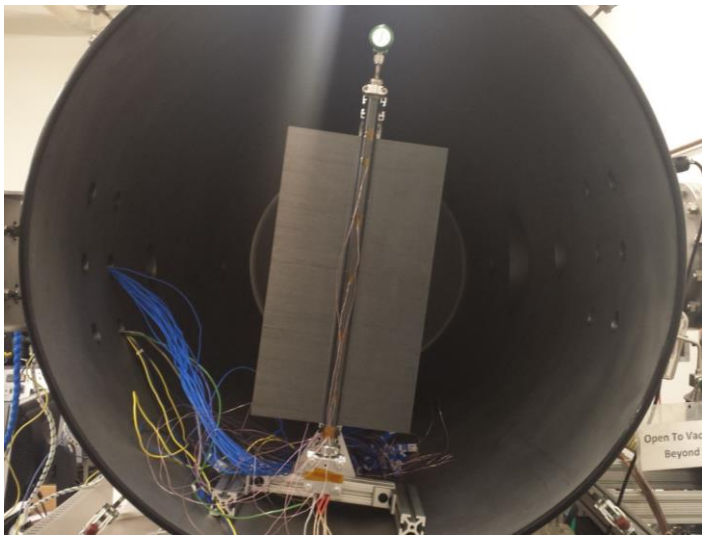

Figure 14. Short heat pipe radiator test fixture instrumented and placed in the vacuum chamber for thermal-vacuum characterization of optimum direct radiator bond to heat pipe.

Each heat pipe was tested in vacuum with a power of 130 W applied and the thermal temperatures along the pipe and radiator were recorded using fourteen thermocouples. To compare the operation of each radiator design, the vapor temperature of each design at 130 W was evaluated. The results from the short heat pipe radiator tests are shown in Figure 15. The best performing radiator design was the 0.2 inch depth radiator, which required a vapor temperature of 116.9°C to reject the 130 W. This was 3°C colder than the 0 inch depth radiator and 2.5°C colder than

the 0.1 inch depth radiator design. As expected, the thermal vacuum testing indicated that the best configuration was the 0.2 in depth radiator. This design provides the largest contact between the radiator and the heap pipe condenser and with a good bond was expected to perform the best.

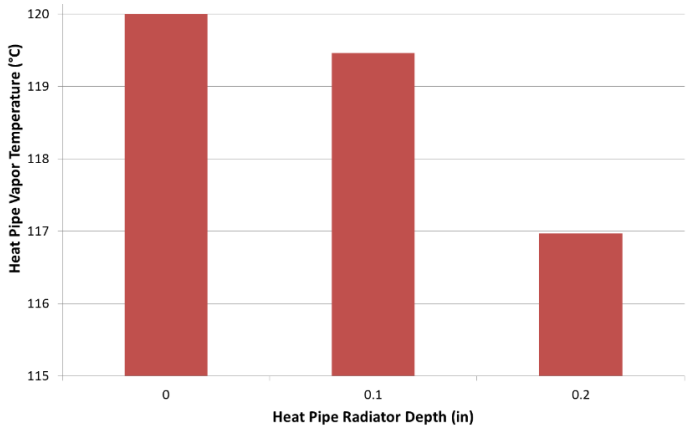

Figure 15. Test results from the short heat pipe radiator design evaluation

Ambient testing was also performed where thermal images could be taken to evaluate the quality of the radiator bond. If there were any problems with the radiator bond, those areas would show up as cold spots in the thermal images. Again, the applied power for the ambient testing was 130W for all the three heat pipe designs.

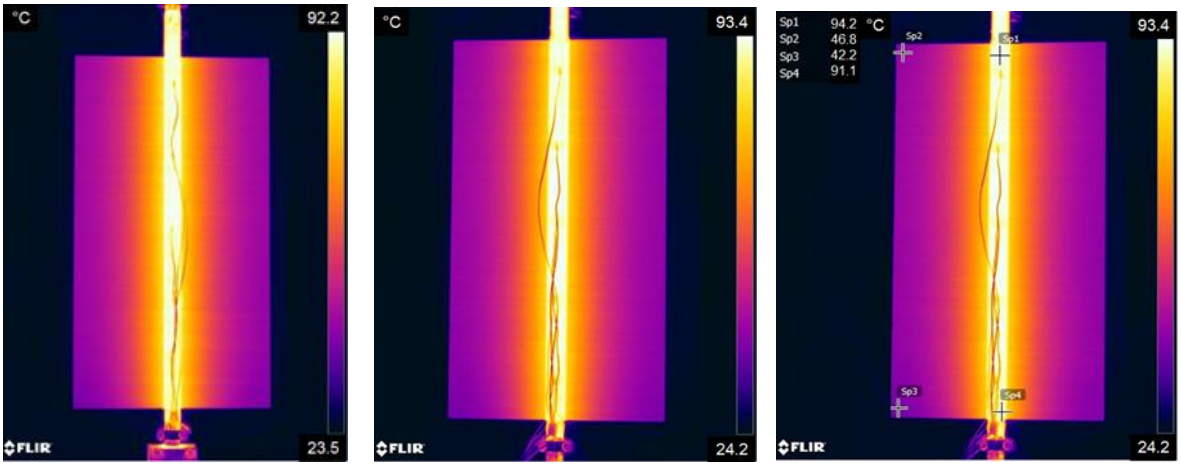

a) b) c)

Figure 16. Thermal Image of a) 0 in, b) 0.1 in and c) 0.2 in depth radiator design

Figure 16 shows thermal images for all three pipes. The thermal image of the 0 in depth radiator is shown in Figure 16a. There were no detectable problems with the radiator bond or the radiator itself. The bond area is shown in the middle as the highest temperature area and is isothermal. There are also no sudden temperature changes along the radiator from the middle to the edges, which indicates that there are no defects in the radiator. Figure 16b shows the thermal camera image of the 0.1 in depth radiator sample. The bonding area is isothermal, with no cold spots that would indicate problems with the radiator bond. The radiator itself also shows no damaged areas in the thermal image. The thermal image for the deepest radiator design, the 0.2 in depth, is shown in Figure 16c. Like the other two radiator designs, the 0.2 depth radiator did not show any problems with the bond or radiator. This depth had the greatest risk due to the depth of the radiator wrap, but there were no problems with the bond. In conclusion the thermal images indicated that the radiator bonding was successful for all the designs and the vacuum tests showed measureable improvement in performance between the 0 in depth and the 0.2 in depth radiator. VST indicated that the 0.2 in depth radiator was not more difficult to manufacture than the other two radiator designs, so manufacturability was not a factor in the down select process. After the testing was complete ACT selected the 0.2 in depth radiator as the design for the module fabrication.

Radiator Heat Pipe Module Develpment

The radiator heat pipe module is a full-scale prototype based on the final design. The purpose of the prototype heat pipe module is to validate the heat transport capability and the ability to start-up from a frozen state.

Module Heat Pipe Test Setup

Figure 17 shows a CAD rendering of the integrated heat pipe and test setup. Figure 17a provides a cut-away of the top portion of the test setup to demonstrate how the condenser is positioned within the cold wall/chiller block assembly. The cold wall/chiller block assembly is made of aluminum and is offset by approximately 1/8 in from the condenser surface. The purpose of the offset is to prevent stresses induced by CTE mismatch between the titanium and aluminum surfaces, and to prevent overly harsh freezing conditions when performing freeze/thaw testing. Figure 17b illustrates the bottom portion of the test setup, which shows the plumbing for flow control and the intrusive RTDs used to determine the power transport of the heat pipe by calorimetry.

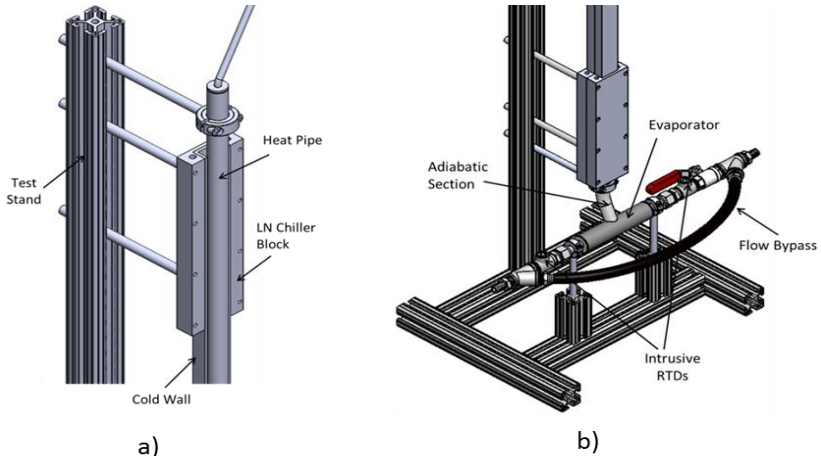

Figure 17. CAD model of test setup top portion a) and bottom portion b)

Figure 18 shows the locations of thermocouples along the heat pipe and cold wall. All thermocouples for the heat pipe were spot welded to ensure a good contact. The three wall thermocouples are located on the outside surface of the cold wall.

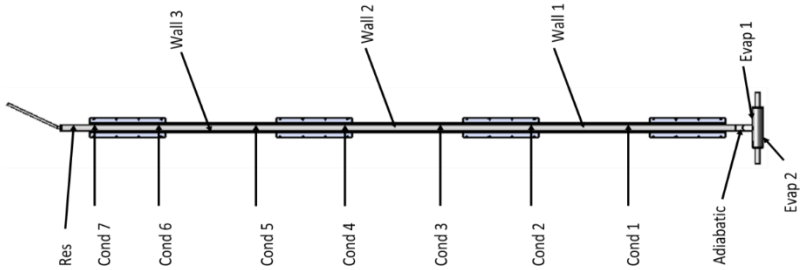

Figure 18. Thermocouple map of heat pipe and cold wall

The fabricated test setup is shown in Figure 19. The hot water supply is pumped by a Sterling temperature control unit (TCU) through heavy-duty rubber hosing. A volumetric flow meter (0-1 GPM) and filter that are mounted upstream of the evaporator heat exchanger inlet. During operation, the pump for the Sterling temperature control unit maintains a constant flow rate of 30 gal/min. In order to regulate the water flow through the evaporator heat exchanger, a by-pass line and two ball valves are installed into the system. Intrusive resistance temperature detectors (RTDs) are used to monitor the coolant temperature at the inlet and outlet of the evaporator manifold. By knowing the water inlet and outlet temperatures and the volumetric flow rate, the power being dissipated by the heat pipe radiator can be determined from calorimetry calculations. Readings from the TC probes and RTDs were directly inputted into a Keithley data-acquisition (DAQ) system for real-time monitoring and data-logging.

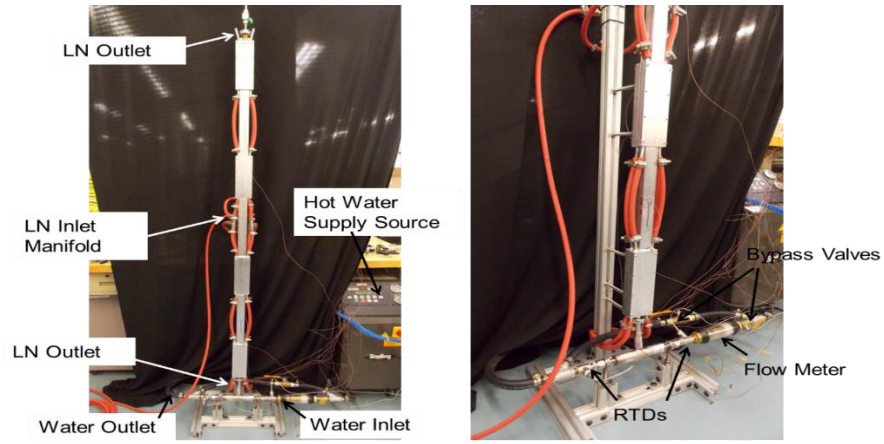

Figure 19. Test setup for heat pipe module thermal performance and freeze/thaw testing

Heat Pipe Module Testing Methodology and Results

Two different types of thermal tests were performed on the heat pipe module to validate proper operation prior to direct bonding. The first test was a thermal performance test to verify temperature uniformity and heat transport capability. The second test was a freeze/thaw test to verify that the accumulation wick design could enable the heat pipe to start up from a frozen state.

For the ***thermal performance test,*** the heat pipe was charged as a CCHP (for simplicity) and varied the amount of power transported by maintaining a constant water supply inlet temperature and adjusting the sink temperature via the cold wall temperature set-point. It was expected that as the sink temperature dropped, the power transported by the pipe would increase.

For the ***freeze/thaw test***, non-condensable gas (argon) was added to the heat pipe to enable start up from frozen conditions. The amount of NCG added to the heat pipe was based on the vapor temperature of the coldest heat pipe in the final radiator design, such that at nominal system conditions (i.e. 127°C inlet, -23°C sink) the condenser of this pipe is fully active and the NCG front is located at the bottom of the reservoir section.

Thermal Performance and Freeze/Thaw Test Results

Figure 20 shows the results for the thermal performance test for three different sink temperature conditions: 30°C, 5°C and -20°C. At first glance, the overall temperature difference along the heat pipe appears somewhat large, ranging between 3-7°C for the highest and lowest sink temperature condition, respectively. However, it was determined that some of the intermediate thermocouples had relatively poor contact and were causing the overall temperature difference to appear artificially large. The actual overall temperature difference between the evaporator and the reservoir surfaces ranged from 2-2.6 for the highest and lowest sink temperature conditions, respectively. This result was considered satisfactory for demonstrating proper heat pipe operation.

The power transported by the heat pipe for each sink condition is also included in Figure 20. Each power was calculated based on calorimetry of the hot water supply by measuring the temperature difference of the fluid across the evaporator HEX and measuring the volumetric flow rate. As expected, the power transported by the heat pipe increases with decreasing sink temperature.

Figure 21a shows the results for the freeze/thaw testing from beginning to end while Figure 21b provides a zoomed view of the same plot to show the VCHP behavior during heat pipe start-up. As the cold wall temperature begins to drop, it was apparent that the condenser TCs 1-6 drop rapidly, while condenser 7 and the reservoir TCs lagged behind. This behavior is partly due to the presence of the NCG, but is also due to the fact that the cold wall does not fully cover this region of the heat pipe. The insufficiently long cold wall was the result of a design oversight, which will be eliminated from future designs. Once the evaporator temperatures were exposed to freezing temperatures for an adequate period of time, the cold wall was shut off and the water supply temperature began ramping up to the nominal operating temperature (~127°C). Approximately 20 minutes after the start of the temperature ramp-up, the heat pipe condenser experienced a rapid increase in temperature. This behavior demonstrated that the condenser was receiving vapor from the evaporator, and is indicative of a successful heat pipe start-up.

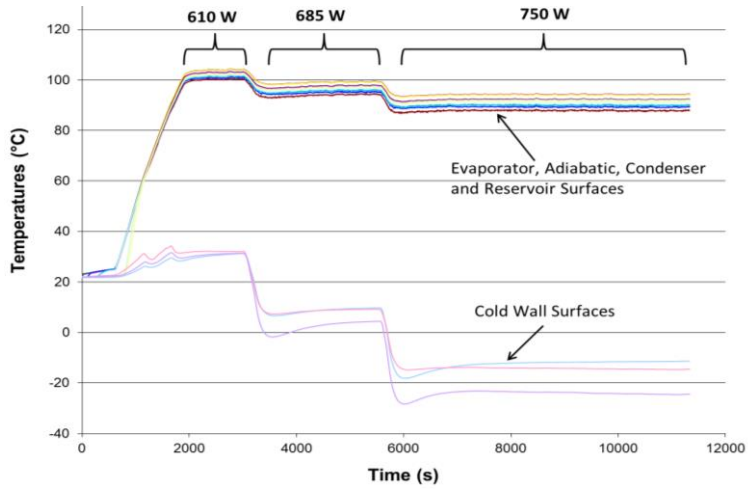

Figure 20. Thermal performance test results for heat pipe module at three different sink temperature conditions

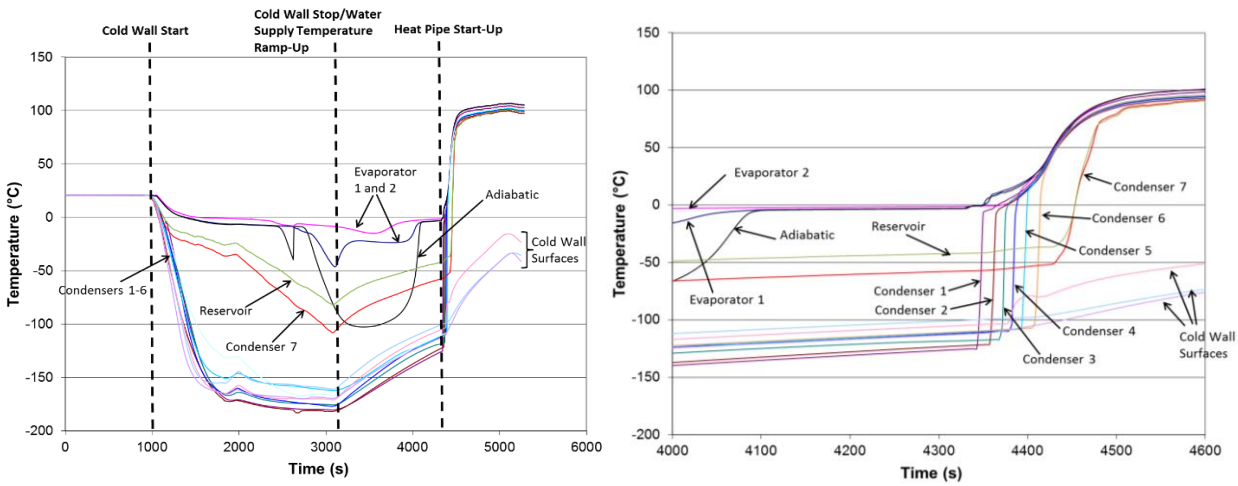

a) b)

Figure 21. a) Freeze/thaw test results for heat pipe module b) Detailed view

IV. Conclusion

The design of the direct bond single face sheet radiator for Surface Fission Power was finalized showing superior specific rejected power when compared to POCO foam based double face sheet radiator. The direct bond procedure and recipe were successfully developed. The systematic experimental study of the wrapping angle between the GFRC face sheet and the titanium condenser shows that the configuration with a depth of 0.2 in (corresponding to the largest wrapping angle) provides the lowest thermal resistance with minimum manufacturing additional risks. Thermal imaging showed temperature uniformity in the bonding area for all three samples. It demonstrates that the direct bonding technique developed by VST is reliable and provides confidence for further large scale manufacturing of the full-scale modular radiator. The heat pipe of a module was tested alone in the presence of a cold wall. The heat pipe rejected 610 W, 685 W and 750 W when the heat sink (cold wall) temperature was 30°C, 5°C and -20°C respectively while the collant temperature was maintained at 127°C. It demonstrated that the heat pipe is ready to be integrated with a GFRC fin as a whole module. The heat pipe architecture (including the bi-porous evaporator) presents thermal resistances that are consistent to the predicted ones used during modeling. The heat pipe was also tested as a VCHP during freeze-thaw cycling demonstrating the startup from a frozen condition. Next step is testing of the fabricated module. As a function of these results, the 12 clusters that form the full scale modular radiator will be fabricated and tested.

Acknowledgments

This research was sponsored by the NASA Glenn Research Center under Contract No. NNX14CC03C. Any opinions, findings, and conclusions or recommendations expressed in this article are those of the authors and do not necessarily reflect the views of the National Aeronautics and Space Administration. Corey Wagner was the technician at ACT for this project.

References

Anderson, W.G., Bonner, R., Hartenstine, J.R., and Barth, J., "High Temperature Titanium-Water Heat Pipe Radiator," STAIF 2006, Albuquerque, NM, February 12-16, 2006, proceedings of Space Technology and Applications International Forum (STAIF-06), edited by M. S. El-Genk, Vol. 813, pp. 91-99, American Institute of Physics, Melville, New York, 2006. http://www.1-act.com/wp-content/uploads/2013/01/SPESIF-2009-VCHP-Radiators-for-Lunar-and-Martian-Environments.pdf

Anderson, W.G., Tamanna, S., Tarau, C., Hartenstine, J.R., and Ellis, D.L., "Intermediate Temperature Heat Pipe Life Tests and Analyses," 43rd International Conference on Environmental Systems (ICES 2013), Vail, CO, July 14-18, 2013a. http://www.1-act.com/intermediate-temperature-heat-pipe-life-tests-and-analyses/

Anderson, W.G., Muzyka, B.J., Peters, C.J., Hartenstine, J.R, Stern, T., and Williams, G., "Variable Conductance Heat Pipe Radiator for Lunar Fission Power Systems," 11th International Energy Conversion Engineering Conference (IECEC), San Jose, CA, July 15-17, 2013. http://www.1-act.com/variable-conductance-heat-pipe-radiator-for-lunar-fission-power-systems/

Briggs, M. H., Gibson, M., and Geng, S., "Development Status of the Fission Surface Power Technology Demonstration Unit," Nuclear and Emerging Technologies for Space (NETS-2015), Albuquerque, NM, February 23-26, 2015.

L. Mason, D. Poston, and L. Qualls, "System Concepts for Affordable Fission Surface Power", NASA Technical Memorandum 215166 (2008).

Mason, L. S., Oleson, S. R., Mercer, C. R., and Palac, D. T., "Nuclear Power System Concepts for Electric Propulsion Missions to Near Earth Objects and Mars," Nuclear and Emerging Technologies for Space (NETS-2012), The Woodlands, TX, March 21-23, 2012.

Maxwell, T, Tarau, C., Anderson, W.G., Wrosch, M, and Briggs, M.H., "Low-Cost Radiator for Fission Power Thermal Control," 13th International Energy Conversion Engineering Conference (IECEC), Orlando, FL, CA, July 27-29, 2015. http://www.1-act.com/wp-content/uploads/2014/08/IECEC-2014-Low-Cost-Radiator-for-Fission-Surface-Power-Systems_Final.pdf

Stern, T., and Anderson, W.G., "High Temperature Lightweight Heat Pipe Panel Technology Development," Space Nuclear Conference 2005, San Diego, CA, June 2005. http://www.1-act.com/high-temperature-lightweight-heat-pipe-panel-technology-development/